Hindawi

Research Article

Image Self-Coding Algorithm Based on IoT Perception Layer

Hao Wu [ID]

International School, Beijing University of Posts and Telecommunications, Beijing 100876, China

Correspondence should be addressed to Hao Wu; 2019213092@bupt.edu.cn

In fact, with the quick growth of IoT-related industries in recent years, multimedia contents such as digital image videos have also shown explosive growth. In the sensing layer of the three-layer IoT architecture, sensors are the most critical part, which mainly sense the state of the environment. In this paper, an image self-coding algorithm based on the IoT perception layer is proposed. There is no specific encoding algorithm for the pictures collected by the current Internet of Things network perception layer. This results in poor search results for the network images collected by the sensor at the perception layer. A deep convolutional neural network image self-coding algorithm based on the IoT perception layer combines prior knowledge with deep involutional aural networks to increase the discriminative ability of images while preserving the message of the images themselves and improving the goal of image search accuracy. The experimental results show that the block search algorithm is used for image registration to reduce energy consumption, the absolute difference sum algorithm is improved to improve the accuracy of image registration, and the progressively out weighted average algorithm is used to stitch the images. After image stitching, the communication volume with the base station is reduced, which can effectively reduce the network load by 60%.

1. Introduction

The IoT is mainly used for the purpose of perception [1, 2]. Like skin, the awareness level can be employed to collect information, identify the messages collected, and evaluate the impact of information interactions on the IoT [3]. They are effectively interconnected at anytime and anywhere but there is a threat of information disclosure to a certain extent. If this situation is not effectively protected, it is likely that the information will be used, thereby harming the legitimate interests of people. The web layer is the brain and information transmission and processing of the nerve center of the Internet of Things [4, 5]. The adoption level is a combination of the "social divide" of the IoT and industry requirements, allowing for a wide range of smarts [6]. Apply level is the intensive blend of IoT and professional technology of industry, combined with industry demand, to achieve industry smartness, which is analogous to human community partition, and finally constitutes human community [7, 8]. The sensing layer is the core of the IoT. It is a vital part of data collection. Through the sensing layer, IoT can realize the sensing of objects [9, 10]. Through the

device's radio frequency identification, sensors, two-dimensional code, etc., it is connected to the wireless network through the interface, thereby giving the object "intelligence" [11]. To enable communication and dialogue between people and things, as well as between organizations, the network that links organizations is known as the " IoT." Therefore, IoT is based on sensor networks. Common sensing layers are RFID, wireless sensor networks, and other sensing devices [12, 13].

The IoT perception layer has information security characteristics. Generally speaking, the node devices of the IoT perception layer have no value. If there are no corresponding protection measures, the system will be persecuted once an intruder invades. Communication systems are very vulnerable to security threats. Intruders can tamper with the information layer of the IoT at will. The existence of a large amount of false information seriously affects the security environment of the IoT [14]. The network layer signal is the main transmission method, but the network environment itself is uncertain. When the nodes of the IoT perception layer work normally, criminals and attackers can use illegal means to steal information from the IoT perception layer. In

addition, criminals can also camouflage their identities to a certain extent. This camouflage is still legal, so it is difficult to perceive the identity problem, and finally to achieve the purpose of stealing IoT user information. Some attackers even use signal bombing to destroy nodes in the IoT perception layer. The information security characteristics of the Internet of Things application layer, because the related power-saving devices are not protected during the operation of the IoT, it is easy to configure information remotely. Tampering with criminals, tampering, and erasing information are the main threats facing IoT systems [15]. Although current IoT information management platforms have corresponding security standards and specific protection measures, there are still hidden dangers in the IoT itself. Both audit security and the security of IoT identity authentication are threatening the normal operation of the IoT. In addition, the problem of human-computer interaction has become more and more obvious, and the reliability of the IoT is threatened. At the application layer, data processing and analysis must be performed. These two aspects will also face security and stability issues during implementation [16].

With the rapid recognition of the concept of the IoT and the strong support of the country, the application of the IoT will continue to expand and deepen. As intelligent nerve endings, the sensing layer will be widely used. Considering the shortcomings of the sensor nodes in terms of energy, computing power, storage capacity, etc., the security of the sensor network is also very challenging. Xing-Yuan Wang presents a new and valid graphical image encryption algorithm using chaos and DNA coding rules [17]. Using the piecewise linear chaotic graph (PWLCM) and logic diagram to generate all the parameters required by the proposed algorithm, DNA coding technology is used as an auxiliary tool. Chen and Guo Tai proposed an efficient encoding algorithm that requires only N bits of memory and has an XOR operation [18]. In addition, auxiliary variables in the algorithm can share memory to reduce additional memory requirements. In addition, a parallel 2 bit encoding algorithm is also proposed to improve encoding throughput. Menassel et al. provide a more detailed study of the wolf pack algorithm for fractal image compression [19]. The entire image is considered as a space search, where the space is divided into multiple blocks, and the scooter wolf explores the space to find other smaller blocks, which are similar to their parameters. taxi wolf read the entire space carefully and chose the most suitable plot. After a fixed number of iterations, or if there is no improvement in the lead wolf solution, the process will stop. When the signal is undersampled along the low bandwidth direction, no aliasing occurs. In this study, Schmidt and Seginer used this feature to divide the SPEN experiment into many interlaced shots, and the inaccuracies of these shots are automatically compared and corrected as part of the navigator-free image reconstruction analysis [20]. This can explain the normal phase noise and the motion of objects during signal collection.

With the development of software radio and cognitive radio technology, research on multisystem communication signal automatic modulation recognition has made much progress and results. Although there are various methods for identifying communication signal modulation methods, modulation recognition is essentially a pattern classification problem. Its identification research content is mainly the extraction of classification features and the design of classifiers. This paper proposes an image self-encoding algorithm based on the perception layer of the IoT. There is no specific encoding algorithm for the pictures collected by the current perception layer of the IoT. This results in poor search results for the network images collected by the sensors of the perception layer. A deep convolutional neural network image self-coding algorithm based on the perception layer of the IoT, combining prior knowledge with the deep convolutional neural network while retaining the information of the image itself, increases the discrimination of the image and improves the image recognition ability. The goal of image search accuracy. Experiments show that compared with other algorithms' objective indicators, the accuracy and average accuracy of the algorithm mean the effectiveness of the algorithm, especially at low coding length.

2. Proposed Method

2.1. IoT Architecture. The IoT is an extension of the traditional network, breaking through the mindset of people-to-people interconnection, and achieving the interconnection between people and equipment, equipment and equipment [21]. The unlimited potential and huge influence of the Internet of Things has aroused widespread concern in academic circles, and research on the Internet of Things has also achieved outstanding results. Following the three-tier architecture of the Internet of Things is a general consensus among academics.

The perception layer uses various types of perception layer devices as antennas to obtain large-scale dynamic and static information in the physical world. Dynamic information includes monitoring environmental changes and behavioral changes. The static information includes the basic situation of the article and the identification of the substance. Due to a large number of devices at the sensing layer, the collection of measurement data by various types of devices is performed in a multidimensional, multiclass, and multi-standard distributed manner, reaching into all directions and all angles of the measurement environment. It requires the coordination of each piece of equipment in processing. Finally, the gateway enables the data in the perception layer to interact with other applications or devices in the network to achieve shared resources [22]. The perception layer includes a sublayer for collecting information, a sublayer for data cooperative processing, and communication technology. The collection information sublayer collects information data in the real environment through various devices of the perception layer. The devices responsible for information acquisition in the perception layer include RFID (radio frequency identification technology), sensors, laser scanning, and multimedia devices. The data cooperative processing sublayer completes the preliminary processing of the

data by coordinating various devices, and removing redundant information in the perceptual data so that the data transmitted by the perceptual layer has higher accuracy and improves transmission efficiency. The middleware of the perception layer solves the heterogeneity problem of the device so that the acquired data can be applied to various applications. The functions implemented include positioning, synchronization, management of devices, code, status, and services. The data sensed by the collected information sublayer is submitted to the data coordination processing sublayer for preliminary processing, and more real and effective intelligence from the physical world is submitted to the network layer.

The main function of the network layer is to transmit data and send the data obtained by the perception layer to the upper-layer applications through the basic network such as the Internet. In addition to the Internet, there are mobile communication networks such as the Broad Grid, TD-SCDMA, Ethernet, Bluetooth, ZigBee and other short-range wireless networks, digital trunking and other dedicated networks, and satellite networks [23]. The network layer needs to solve the related problems of communication transmission. The perception layer transmits the redundant data to the network layer, and the network layer performs protocol conversion on it and selects a better routing line for forwarding so that the target device can receive the data smoothly. The Internet of Things network layer is composed of two types of networks: access networks for multiple heterogeneous network connections and transmission networks for information interaction. The network layer of the IoT encompasses almost all current network types, creating a connection, that is, larger than the Internet. In order to achieve information exchange in the IoT, data needs to be routed by multiple types of networks [24]. And due to the different technical characteristics of heterogeneous networks, the communication formats and protocols used are inconsistent. How to achieve complete and accurate high-quality interaction is the main problem to be solved at the network layer. At the same time, massive information is generated at any time on the Internet of Things, which poses higher challenges to the transmission bandwidth of the network layer and the processing capacity of the gateway. The main concern of the IoT network layer is how to reduce the impact of network bandwidth with the development of the IoT and break through the bottlenecks encountered in the transmission of IoT gateways.

The application layer of the IoT determines the functions that the IoT system should have, while setting requirements for IoT services. The application layer mainly includes an application classification layer and a service-providing layer. The application classification layer analyzes various application requirements, mines common characteristics among them, and recombines similar application requirements into application subsets. The service provider layer is mainly responsible for providing data support for application requirements and uses the raw data collected by the perception layer in real-time to dynamically update the data resource library. The IoT application layer is mainly responsible for the development and utilization of raw data. The IoT application layer processes and controls the massive information transmitted in the network layer in a timely manner, including the classification and integration of data, processing calculations, and data mining. The IoT application layer meets the actual application needs of various industries and provides service support for smart homes, meteorology, environmental monitoring, logistics, public safety, telemedicine, etc. It is a service program or system software that provides an information interaction platform for different system applications. The IoT middleware exists independently in the IoT, and it integrates functions that can be shared by applications for use. According to the differences in design goals, IoT middleware can be divided into three categories: remote procedure call middleware, message-oriented middleware, and object request proxy middleware. The application of the Internet of Things has become a research hotspot, and several typical applications such as health monitoring, intelligent transportation, and telemedicine have been put into use to provide services for people. Cloud computing is also an important part of the application layer. The cloud can accommodate the massive data of the Internet of Things, and the data can be analyzed and processed through cloud computing.

2.2. Deep Learning. Deep learning is a very popular research direction in the field of machine learning in the past decade. It is equivalent to the second wave of machine learning, and the first time is shallow learning corresponding to deep learning. The difference between them is mainly two points: one is the depth of the model, and the other is that deep learning highlights the importance of feature learning. In traditional machine learning, because the original data is very large and complex, it is very difficult to process. In many cases, it is necessary to rely on experience and spend a lot of time and energy to extract features from the original data. Therefore, researchers have to think about how to design a feature extraction method for machine learning systems and convert the original data into corresponding internal feature representations. Deep learning theory came into being. The essence of deep learning is to build a machine learning model with more hidden layers, learn more effective feature representations from a large number of original data samples, extract more accurate features of these data, and improve the accuracy of prediction models or classification models. Sex. The basis of deep learning is that massive data is needed for training. Only in this way can we learn more robust features.

Restricted Boltzmann machine (RBM) is a stochastic neural network model based on statistical mechanics. RBM has two layers of structures, namely, the hidden layer and the visible layer. There is a full connection between layers, there is no connection in the layers, and there is no self-feedback. This energy function-based model is called an energy model, and the energy model is used to solve the solution when the network is most stable as the target solution. The energy function formula of the RBM model is defined as follows:

$$E(v, h|\theta) = -\sum_{i-1}^{n} \sum_{j=1}^{m} w_{ij} h_i v_j - \sum_{j=1}^{m} b_j v_j - \sum_{i=1}^{n} a_i h_i. \quad (1)$$

State w_{ij} represents the connection weight between the j-th unit of the hidden layer and the i-th unit of the visible layer, a_i represents the offset of node i in the hidden layer, and b_j represents the offset of node j in the visible layer. From formula (1), we can see that there is an energy connection between each visible layer node and the hidden layer node. Based on formula (1), when all parameters are determined, the joint probability distribution of (v, h) can be obtained:

$$P(v, h|\theta) = \frac{e^{-E(v,h|\theta)}}{Z(\theta)},$$

$$Z(\theta) = -\sum_{v,h} e^{-E(v,h|\theta)}. \quad (2)$$

Here, $Z(\theta)$ is the normalized molecule and $P(v, h|\theta)$ is called the Boltzmann distribution function. For the distribution $P(v|\theta)$ of observation data v, that is, the probability that the RBM model assigns to the node v in the visible layer is

$$P(v|\theta) = \frac{1}{Z(\theta)} \sum_{h} \exp(-E(v, h|\theta)). \quad (3)$$

Due to the special nature of the RBM model mechanism, the activation status of the nodes between the hidden layer and the visible layer itself are conditionally independent, that is,

$$P(v|h) = \prod_{i=1}^{n} P(v_i|h),$$

$$P(h|v) = \prod_{j=1}^{m} P(h_j|v). \quad (4)$$

When the node status of the visible layer is given, the probability of the j-th hidden layer node activation is

$$P(h_j = 1|v, \theta) = \sigma\left(b_j + \sum_j v_i W_{ij}\right), \quad (5)$$

where $\sigma(\cdot)$ is the sigmoid activation function, and the expression is

$$\sigma(x) = \frac{1}{1 + \exp(-x)},$$

$$P(v_i|h, \theta) = \sigma\left(a_i + \sum_j h_j W_{ij}\right). \quad (6)$$

It was discovered that the cat's cerebral cortex has been studied and a special network structure was found that reduces the complexity of the feedback neural network. Call it Convolutional Neural Network (CNN). After decades of development, CNN has been widely used in image classification, face recognition, and other directions. The entire network structure of CNN is composed of multiple convolutional layers and downsampling layers. Among them,

each layer is composed of many two-dimensional planes, and there are many independent neurons in these two-dimensional planes. In addition, the CNN model also incorporates three structural methods: local receptive field, spatial downsampling, and weight sharing. The local receptive field indicates that neurons in a layer in the network model are only connected to neurons in the local domain of the previous layer, and are not connected to neurons outside the domain. This connection method greatly reduces the number of weights that need to be trained.

Spatial downsampling can reduce the resolution of the feature map and reduce the dimension of the feature map. When downsampling in CNN, the method of pooling was selected, that is, the maximum value or average value was calculated for a certain area of the feature map, and these values were used to represent this area. This method reduces the computational dimension and effectively prevents overfitting. Weight sharing refers to the use of a convolution kernel to convolve neurons in all hidden layers, that is, the method of extracting certain features in the same feature map is the same. You can use the same method in the image. Different regions are extracted, which greatly reduces the network parameters and improves the operation speed. Compared with other deep learning models, the CNN model also has different activation functions. The currently popular ReLu is used instead of the sigmoid function. Because in other neural network models that use the sigmoid function as the activation function, if the network is not pretrained, it may appear that it cannot converge or the gradient disappears when calculating the gradient. But general pretraining is difficult to get a satisfactory result, so we need to take some sparse processing measures on the output data. However, the output of the sigmoid function is not sparse, and the ReLu function will solve this problem. The specific formula is

$$g(x) = \max(0, x). \quad (7)$$

It can be seen from formula (7) that if the calculated value is less than 0, the final result will be forced to 0, and the remaining values will remain unchanged.

2.3. Autoencoder. Autoencoder (AE) is a neural network model, that is, trained using unsupervised training methods. It uses the back-propagation algorithm to estimate the parameters of the network model so that the target output value is equal to the input value, that is, using self-encoding the learner learns an identity function. The AE network model contains only one hidden layer, the bottom layer is the input layer, and the last layer is the output layer. After going through this reconstruction process, the hidden layer of the AE network model can retain the features necessary for reconstructing the input original data.

When the input vector is x, the vector a is obtained through the first layer network:

$$a = f(Wx + b). \quad (8)$$

We get the vector y after going through the second layer network:

$$y = f(Wa + b),$$

$$\left[\theta^*, \theta'^*\right] = \arg_{\theta, \theta'} \min \frac{1}{n} \sum_{i=1}^{n} L(x_i, y_i). \tag{9}$$

Here, the parameters $\theta = \{W, b\}$, $\theta' = \{W', b'\}$, and L is the traditional error loss function:

$$L(x, y) = x - y^2. \tag{10}$$

The method for solving the optimal solution of model parameters is the commonly used stochastic gradient descent method. In the AE network model, the number of nodes in the hidden layer can be less than the dimension of the input sample, or the number of input nodes can be much larger. When the number of nodes in the hidden layer is less than the number of input nodes, the AE network at this time is used to reduce dimension, when the number of nodes in the hidden layer is greater than the number of nodes in the input layer, you can add a sparseness limit to the nodes in the hidden layer to suppress the activation values of some nodes so that the internal structure of the sample training set can be better discovered and sparse. This kind of autoencoder with sparse restriction is called sparse autoencoder (SAE). In order to make the hidden layer unit of the AE network model able to learn more robust features, it has a better anti-noise ability to the input data. Researchers have proposed a noise reduction autoencoder (DAE). This network model adds random noise to the sample training data at the input layer and reconstructs the sample training data without noise at the output layer. After a large amount of training, the DAE network model can still obtain the original sample training data without adding noise. This is because after the original sample training data is added with noise, the DAE model can obtain more stable and standardized features in the training data, which lays a good foundation for later classification and recognition.

In order to overcome the disadvantages of traditional image coding methods in processing the images of the perception layer of the Internet of Things, this study proposes a novel social network image encoder algorithm. The algorithm uses pretrained models to extract features, then uses the K-means algorithm to obtain distance information between features, and uses the characteristics of social networks on the same Weibo to correct the distance information of images. Then use the deep convolutional neural network to learn the distance information of the picture, extract the fully connected layer in the deep convolutional neural network as the encoding, repeat the above steps, and get the final image encoding. Using this algorithm, social network images can be effectively encoded. The final image encoding retains both its own image characteristics and the prior knowledge of social networks. This article first preprocesses the initial image, then corrects the distance information of the extracted image based on the prior information of the existing social network image, and then uses a deep convolutional neural network to learn the corrected image distance information. This step can do multiple loops; finally, perform sparse auto-encoding

according to the number of self-encoded bits. After the coding network is trained, the untrained social network images can be coded through a deep convolutional network to find approximate images in the social network image library, and then the objective evaluation index is used to evaluate the effectiveness of the coding.

3. Experiments

3.1. Experimental Data. Experiments are performed with the algorithm as the core. In order to test and verify the improved algorithm, two sets of data are used for testing, including the public database STL-10 and the self-built image database. In the STL-10 database experiment, the sample dimension of the sparse autoencoder is $8 * 8$, that is, the size of the convolution kernel in the first convolution layer of the convolutional neural network is $8 * 8$, and the sample set includes 100,000 $8 * 8$ samples.

3.2. Extraction of Image Distance Information. First, extract the preliminary features of the image, and then cluster and process the preliminary features. This section gives the first step of the DCNNSE algorithm. Use $I = \{I_1, \ldots, I_{ns}\}$ to represent the input n_s images, which mainly include the following 4 steps:

(1) For all images, use the VGG-16 model to extract features. Each picture is mapped to a vector of 4096 dimensions. Use the K-means algorithm to cluster the image features, and assign a label $y = \{y_1, \ldots, y_{ns}\}$ to each image. The number of clusters is selected as shown in

$$\text{classes}_i = \left[4096 \times \left(\frac{l}{4096} \right)^{i/2} \right]. \tag{11}$$

(2) According to the prior condition that the content of the same Weibo picture belongs to the same topic, it is necessary to adjust the problem of tagging pictures with different tags under the same Weibo topic. Assume that there are two types of results a_i and b_i, and these two categories are not the same, and it is known that a_1 and b_2 are two pictures under the same Weibo when data are acquired. Feature average under the blog is

$$\overline{F} = \frac{\left(\sum_{i=0}^{m} F_i \right)}{m}, \tag{12}$$

where m is the number of pictures included in the same Weibo.

(3) Calculate the distance between the feature average and each cluster center, and then classify all the pictures under this Weibo to the nearest cluster center. As shown in equation (13), let the class center of the i-th cluster is center_i.

$$y = \arg_i \min \overline{F} - \text{center}_{i2}. \tag{13}$$

(4) Determine the new clustering center according to the new image label, and use the arithmetic average of the images of the respective categories as the new clustering center, where the count is a statistical function to count the images belonging to the i category.

$$\text{center}_i = \frac{\sum_{i=1}^{ns} F_{y=i}}{\text{count}(y = i)}. \qquad (14)$$

After the above steps, a fine-tuned image clustering label is obtained. In this step, the image distance information of the prior knowledge of the social network is mainly obtained and referenced so that the next learning can be performed so that the learned image not only retains the original image information but is also more differentiated.

3.3. Model Optimization Based on the Internet of Things.

In the aggregated core node of an embedded multicore SoC, blocking occurs if the mission snubber volume is filled and happens when the next mission is reached, while the implementation nucleus has not yet finished the ongoing mission. The chokepoint chance of blocking can therefore be roughly balanced by the probability of the junction snubber being filled.

The graphical depiction of the link between the chance of the pitch count being filled and the mission count is illustrated in Figure 1. With an addition to the mission staging volume, the chance of the staging being filled for each individual mission starts to decline rapidly. As soon as the volume of the mission snubber reaches more than 4, the rate of descent commences slackening. When the mission staging volume of 8 is achieved, the mission staging volume is added again, and the probability that the caches of Core1 and Core2 are full will no longer change; The probability of Core3's cache being full has been lower than 0.2, while the probability of Core4 and Core5's cache being full has approached zero.

Based on the performance assessments shaped by the scheduled network of integrated multicore SoCs, the reaching ratios of each implementation kernel for missions of varying prioritization are available. As Core2~5 take up essentially a similar level of hardware resources, they also have essentially the same mission coping power. If the workload of individual kernels varies considerably, the handling ability of the whole setup will not be very great, so an intelligent method of arranging tasks is necessary. Figure 2 illustrates the allocation of attendance rates per implementation core before and after the use of the automatic allocation and transitions in the practical trials. As can be observed, with the introduction of adaptable sequencing to Core1, the distributed tasks of Preferred 1 and Preferred 2 on Cores 2–5 are better equilibrated.

Figure 3 presents the delivered percentage of parcels between the pathway and the origin junction for three distinct conditions. As can be noticed from the graph, the package delivered rate among gateways and source nodes
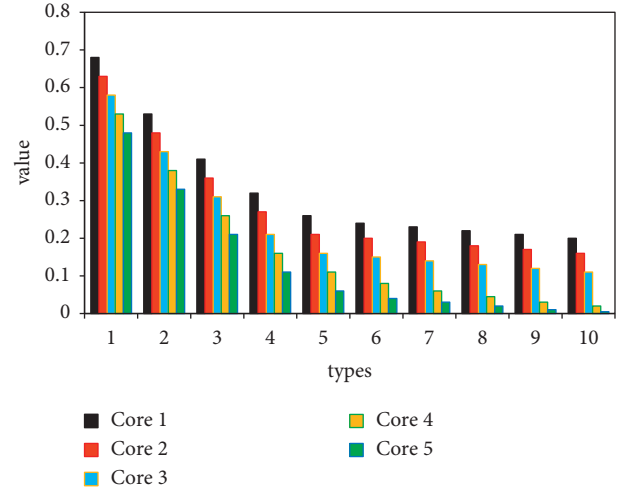

FIGURE 1: The graphical depiction of the link between the chance of the pitch count being filled and the mission count.
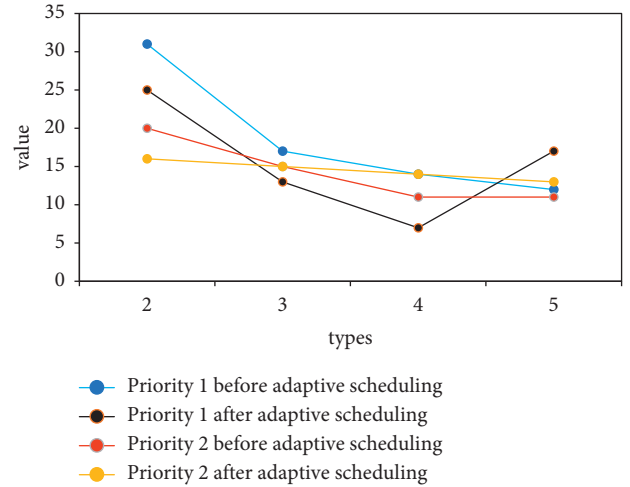

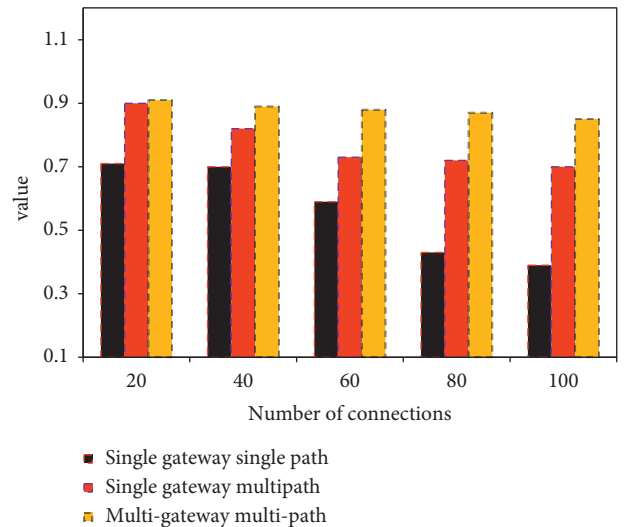FIGURE 2: Comparison of task reach rate before and after adaptive scheduling.

FIGURE 3: The packet delivery rate between the gateway and the source node.
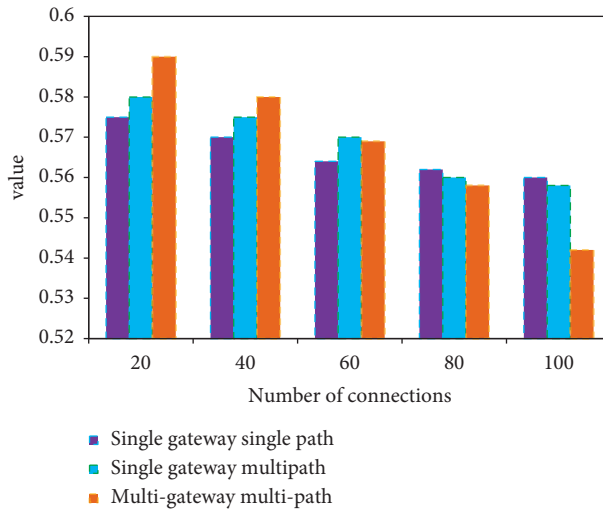
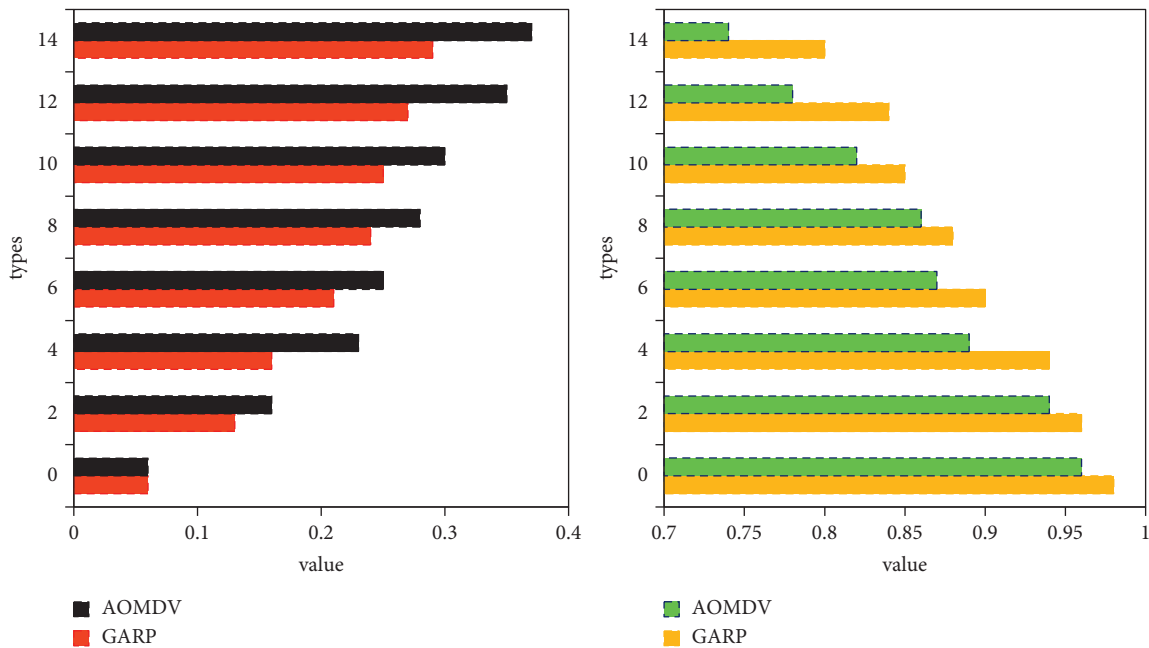FIGURE 4: The comparison of gateway and source node parameters.

FIGURE 5: The comparison of average end-to-end delay between gateway and source node and comparison of packet delivery rate.

falls with the growing number of infections in the three various cases, but at opposite rates. In a uni path delivery approach involving just one gateway, the packet delivery ratios across the gateway and the originating node are the minimum. As can be seen in Figure 4, the network overhead argument in the process of delivery between the gatekeeper and the root node varies with the number of connections in the three cases mentioned above. As can be noticed from the graph, the grid overhead for the three transport options of gateways and origin knots reduces as the count of junctions keeps growing. However, the networking costs of the gatekeeper and origin node trend down as the number of network junctions grows in the multigateway delivery approach and in the multilateral gateway submission approach that uses one carrier alone for transfers.

In particular, the magnitude of the rate of change in the position of the IoT Perception Level knots dictates the rate of change in the terrain of the IoT Perception Level roof and directly indicates the reliability of the IoT Perception Level. During the simplification in this paper, the rate of variation of the mobile locations of the IoT signaling level knots is programmed from 0 m/s to 35 m/s in respective multiplication steps of 5 m/s. During this phase of continuous evolution, the routing agreements GARP and ODTM, the access-oriented version of the gateway-access routing protocols suggested in this paper, both exhibit degraded levels of behavior.

A more detailed analysis of the estimated average end-to-end delay across the gateway and source junction for varying node position change rates is presented in

TABLE 1: The PSRN of the three images changes with the value of k.

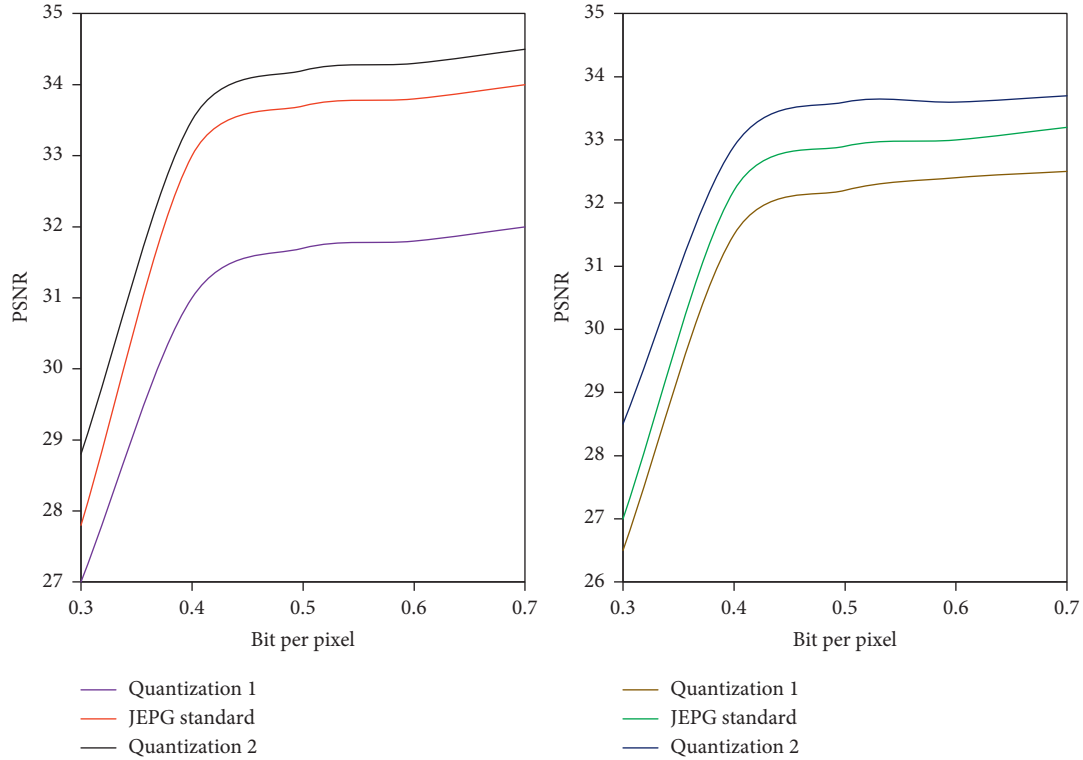| k value	1	2	3	4	5	6	7
Lena	23	27	31	32	33	33	33
Window	21	22	24	26	27	27	27
Beach	25	27	31	33	34	34	34

FIGURE 6: PSNR of Lena image (a) and Peppers image (b) using three quantization tables.

Figure 5(a). The average end-to-end delay between the gateway and the source node for both the gateway-oriented routing protocols GARP and ODTM protocols grows to the different extent as the rate of variation in node position changes. That's due to the fact that the speed, at which node positions become more variable, the network topology shifts much more violently, leading to regular link breakdowns and outages. As a result, the amount of reboots in the process of route finding adds to the overall average end-to-end latency across gateways and origin points. Figure 5(b) indicates a carve-out compared to the delivered rate of packets across gateways and source knots for varying rates of the shift in node placement. The handover rate of traffic between gateways and source knots for the routing agreements GARP and ODTM declines as the change rate of knot positions grows. This is due to the added velocity of knot position variations resulting in formerly formed contacts remaining invalid and losing packs getting heavier and heavier. However, under identical circumstances, the gateway-oriented routing protocol GARP has a marginally lesser amount of packet drop. The reason for this is that aggregation and head selection methods adapted for portal election take into calculation the power of the grid, and the power of the chosen cluster head will not be reduced.

Datagrams are carried among cluster head joints with greater power, which decreases the number of cases, where cluster head joints throw away datagrams due to poor power.

In the multigateway multipath delivery style, the example of the average end-to-end latency between the gateway and the source junction is greater than in the first two situations, when the burden is slight. The main reason for this is that a limited amount of gateways must be picked from the selection of potential tuples, which adds to the traffic latency. However, the usefulness of this approach becomes apparent as the network load becomes heavier as the number of connections increases. At this point, the amount and mass of gateways are available in an efficient and justifiable manner, thanks to the multigateway multipath transmission method. The median end-to-end delays across the gateway and origin junction are less than adding the first two cases, as the superior behavior of the chosen paths is enhanced by this approach and the load is finely balanced than in the first two situations.

3.4. Image Self-Encoding Based on the Perception Layer of the Internet of Things. WMSN's base station collects image data captured by wireless video nodes. There is a trade-off

TABLE 2: The image quality and the number of images that can be transmitted per second at different compression rates.

Compression ratio	Image quality (%)	Frame rate
Q0	2.7	9.98
Q1	3.6	7.72
Q2	4.9	5.58
Q3	6.9	3.98
Q4	8.9	3.12
Q5	28.8	1.56

TABLE 3: The comparison of the size of the change detection image and the original image.

Image number	Full frame size (k)	Test results (k)	Ratio of test result to full frame size (%)	PANR
01	51.8	6.13	11.64	24.78
02	46.6	6.15	12.8	25.87
03	47.6	5.21	11.32	27.89
04	47.4	4.72	9.98	28.97

TABLE 4: The comparison of main parameters of image coding.

Decomposition level	Number of bit planes	Compression ratio	PSNR	Execution time	Service type
3	4	41.9	21.1	Low	Low image quality and short response time
3	5	23.1	26.9	Middle	Low image quality, medium response time
3	6	18.1	30.8	High	Medium image quality, long response time
3	7	16.2	34.2	High	High image quality and long response time

between image quality and maximum network life cycle. If high-quality images are required, the maximum network life cycle must be compromised. On the other hand, if the required image quality is low, the network will have a longer life cycle. The maximum achievable network lifetime is obtained, when there are no transmission errors.

For the purpose of profiling the correlation among capturing flexibility, picture quality, and performance of data sources, some simulation experiments were carried out on MATLAB. Table 1 shows how the signal-to-noise ratio PSRN of three images using JPEG encoding varies with the value of k. Obviously, the amount of DCT multiplication, addition, and memory access operations increases with the increase of k, which makes the energy consumption of image compression also increase. The test images Lena, Window, and Beach have various settlements. Window stands for an image containing a wealth of experience and is categorized as a hightech picture containing more detail at greater depths. Beach represents an image containing smaller amounts of detail and can be classified as a preference for upper-level images containing lower-levels of detail. Beach stands for an image containing less information and can be classified as a low-frequency image containing a low-level of detail.

The quantization step size of JEPG largely determines the rate-distortion performance of the encoded image. The use of the JEPG standard quantization table is often not optimal, because it does not consider the image content. Therefore, in WMSN, the quantization table should be adjusted adaptively according to the scene activity. Here we compare the effects of three quantization tables on PSRN. The JEPG standard refers to the quantization table used in the coding standard.

Quantization 1 refers to the quantization table used in stationary scenes. Quantization 2 refers to the quantization table used in sports scenes. The quantization simulation results of Lena and Peppers images are shown in Figure 6.

Table 2 shows the impact of compression rate on compressed image quality and image quality on frame rate. It can be seen that if the compression rate increases, the image increases but the call rate decreases significantly.

The node cannot fulfill the data transfer assignment and will consume a large amount of power. Following notification of variations, just the mobile object is preserved. As shown in Table 3, the image size of each frame of the detection result is about 5 kb, which is considerably tinier compared to the raw version.

The required model parameters are obtained through simulation experiments, and the performance of the proposed algorithm is evaluated. In order to analyze the relationship between image quality, energy consumption, and data rate, some simulation experiments were carried out. The quantization level and the allowable transformation level for different communication distances and image quality are selected through simulation experiments. The image quality decreases with the increase of the quantization level so the energy consumption of image compression also increases. Energy consumption will increase with the increase of the transformation level, communication distance, and data transmission rate. The adaptability of image transformation to network conditions and service quality is studied by analyzing image coding parameters. By analyzing the network life cycle, and memory allocation, select the appropriate compression rate and image quality. The experimental data is shown in Table 4.

In view of the situation where WMSN is composed of multiple low-performance wireless video nodes, users have high requirements for image quality. Research the image stitching algorithm that WMSN is suitable for, stitch multiple low-resolution images into high-resolution images, remove the information redundancy between nodes, and save resources. An image mosaic algorithm suitable for wireless multimedia sensor networks is proposed. Use block search algorithm for image registration to reduce energy consumption, improve absolute difference and algorithm to improve the accuracy of image registration, and use the weighted average algorithm of gradual and gradual to stitch the images, after the image stitching, the communication volume with the base station is reduced, which can effectively reduce the network load by 60%.

4. Discussion

Due to the limitations of WMSN in terms of energy, calculation, and storage, multimedia data and especially video data, must be compressed and encoded before transmission, reducing the amount of data transmission to save energy. The contradiction between the limited resources and the user's requirements for the quality of service required by the application has become an obstacle to the development of practicality. In order to achieve the goal of saving resources and ensuring the quality of service, this paper conducts an in-depth study on the image coding algorithm. An energy-efficient JPEG2000 image coding algorithm suitable for wireless multimedia sensor networks is proposed. According to network conditions and image quality constraints, a look-up table is used to select the appropriate quantization level and wavelet transform level to reduce energy consumption. A semi-reliable scheme is used for image transmission, and the node decides to forward or discard it according to the remaining energy and data priority.

5. Conclusions

This chapter studies the image communication performance of wireless video nodes based on DCT and DWT in WMSN, and models and analyzes the energy consumption and image distortion in the image encoding and transmission process under resource-constrained conditions. Then an energy-efficient resource allocation scheme is proposed, which adaptively adjusts the complexity of the encoder according to the activity of the monitoring scene. Under different coding complexity, simulation experiments were carried out on different input images. The results show that the proposed resource optimization scheme effectively saves energy at the cost of smaller image quality and transmission data rate loss. At the same time, an energy-efficient JPEG2000 image encoding algorithm suitable for WMSN is proposed. According to network conditions and image quality constraints, a look-up table is used to select the appropriate quantization level and wavelet transform level to reduce energy consumption. A priority-based scheme is used for image transmission, and the node decides to forward or discard it according to the remaining energy and data

priority. The evaluation demonstrates that the suggested approach allows for an important reduction in the computational and commercial energy consumption of the embedded components of the wireless, while maintaining the required image quality.

The method proposed in this paper can indeed have a positive impact on image registration to a certain extent, but there are still many shortcomings in this paper. The application research of human-computer interaction technology is still in the preliminary stage. In future work, it will be based on the existing technology and level are analyzed from more angles, and the quality of research work is continuously improved.

Data Availability

No data were used to support this study.

Conflicts of Interest

The author declares no conflicts of interest regarding the publication of this article.

References

[1] F. Uysal, E. Kilinc, H. Kurt, E. Celik, M. Dugenci, and S. Sagiroglu, "Estimating seebeck coefficient of a p-type high temperature thermoelectric material using bee algorithm multi-layer perception," *Journal of Electronic Materials*, vol. 46, no. 8, pp. 4931–4938, 2017.

[2] M. A. Razzaque, M. Jevric, A. Palade, and S. Clarke, "Middleware for Internet of things: a survey," *IEEE Internet of Things Journal*, vol. 3, no. 1, pp. 70–95, 2016.

[3] Y. Wang, Y. Wang, D. Yu, J. Yu, and F. C. M. Lau, "Information exchange with collision detection on multiple channels," *Journal of Combinatorial Optimization*, vol. 31, no. 1, pp. 118–135, 2016.

[4] H. Al-Zubaidy, J. Liebeherr, and A. Burchard, "Network-layer performance analysis of multihop fading channels," *IEEE/ACM Transactions on Networking*, vol. 24, no. 1, pp. 204–217, 2016.

[5] N. J. Guliyev and V. E. Ismailov, "A single hidden layer feedforward network with only one neuron in the hidden layer can approximate any univariate function," *Neural Computation*, vol. 28, no. 7, pp. 1289–1304, 2016.

[6] A. Futamura, A. Shiromaru, T. Kuroda et al., "Clocks, behavior, and cognition," *Brain and nerve = Shinkei kenkyū no shinpo*, vol. 69, no. 6, pp. 639–649, 2017.

[7] Y. Xue, Y. Zhang, Y. Liu et al., "Scalable production of a few-layer MoS2/WS2 vertical heterojunction array and its application for photodetectors," *ACS Nano*, vol. 10, no. 1, pp. 573–580, 2016.

[8] H. R. Lee, S. W. Lee, C. Shikili, J. Kang, S. Lee, and K. C. Park, "Enhanced electron emission of paste CNT emitters with nickel buffer layer and its X-ray application," *Journal of Nanoscience and Nanotechnology*, vol. 16, no. 11, pp. 12053–12058, 2016.

[9] F. C. Sangogboye, K. Arendt, A. Singh, C. T. Veje, M. V. Kjærgaard, and B. N. Jørgensen, "Performance comparison of occupancy count estimation and prediction with common versus dedicated sensors for building model predictive control," *Building Simulation*, vol. 10, no. 6, pp. 829–843, 2017.

[10] A. Tijou, G. Rosi, P. Hernigou, C. H. F. Lachaniette, and G. Haïat, "Ex vivo evaluation of cementless acetabular cup stability using impact analyses with a hammer instrumented with strain sensors," *Sensors*, vol. 18, no. 2, p. 62, 2017.

[11] S. Wang, S. Zhang, R. Ma et al., "Remote control system based on the Internet and machine vision for tracked vehicles," *Journal of Mechanical Science and Technology*, vol. 32, no. 3, pp. 1317–1331, 2018.

[12] S. Xi, C. Wu, and L. Jiang, "Super resolution reconstruction algorithm of video image based on deep self encoding learning," *Multimedia Tools and Applications*, vol. 78, no. 4, pp. 4545–4562, 2019.

[13] M. Z. Rafique, M. N. Rahman, N. Saibani, and W. ArsadSaadat, "RFID impacts on barriers affecting lean manufacturing," *Industrial Management & Data Systems*, vol. 116, no. 8, pp. 1585–1616, 2016.

[14] W. Wu, J. Wang, and X. Wang, "Online throughput maximization for energy harvesting communication systems with battery capacity," *IEEE Transactions on Mobile Computing*, vol. 16, no. 1, p. 1, 2016.

[15] G. Hua, Y. Zhang, J. Goh, and V. L. L. Thing, "Audio authentication by exploring the absolute-error-map of ENF signals," *IEEE Transactions on Information Forensics and Security*, vol. 11, no. 5, pp. 1003–1016, 2016.

[16] I. I. Livshitz, "A method for optimizing the integrated management system Audit program," *SPIIRAS Proceedings*, vol. 5, no. 48, p. 52, 2016.

[17] X. Wang and C. Liu, "A novel and effective image encryption algorithm based on chaos and DNA encoding," *Multimedia Tools and Applications*, vol. 76, no. 5, pp. 6229–6245, 2016.

[18] G. T. Chen, Z. Zhang, C. Zhong, and L. Zhang, "A low complexity encoding algorithm for systematic polar codes," *IEEE Communications Letters*, vol. 20, no. 7, p. 1, 2016.

[19] R. Menassel, B. Nini, and T. Mekhaznia, "An improved fractal image compression using wolf pack algorithm," *Journal of Experimental & Theoretical Artificial Intelligence*, vol. 30, no. 3, pp. 429–439, 2018.

[20] R. Schmidt, A. Seginer, and L. Frydman, "Interleaved multishot imaging by spatiotemporal encoding: a fast, self-referenced method for high-definition diffusion and functional MRI," *Magnetic Resonance in Medicine*, vol. 75, no. 5, pp. 1935–1948, 2016.

[21] Y. Sun, H. Song, A. J. Jara, and R. Bie, "Internet of things and big data analytics for smart and connected communities," *IEEE Access*, vol. 4, pp. 766–773, 2016.

[22] Z. Lv, Y. Han, A. K. Singh, G. Manogaran, and H. Lv, "Trustworthiness in industrial IoT systems based on artificial intelligence," *IEEE Transactions on Industrial Informatics*, vol. 17, no. 2, pp. 1496–1504, 2021.

[23] Q. Liu, S. Sun, B. Rong, and M. Kadoch, "Intelligent reflective surface based 6G communications for sustainable energy infrastructure," *IEEE Wireless Communications Magazine*, vol. 28, no. 6, 2021.

[24] S. Wan, "Topology hiding routing based on learning with errors," *Concurrency and Computation: Practice and Experience*, vol. 34, 2020.